

Cite this: *Phys. Chem. Chem. Phys.*, 2011, **13**, 8175–8179

www.rsc.org/pccp

PAPER

Differential cross sections for $\text{H} + \text{D}_2 \rightarrow \text{HD}(v' = 2, j' = 0, 3, 6, 9) + \text{D}$ at center-of-mass collision energies of 1.25, 1.61, and 1.97 eV

Nate C.-M. Bartlett,^a Justin Jankunas,^a Tapas Goswami,^a Richard N. Zare,^{*a} Foudhil Bouakline^b and Stuart C. Althorpe^c

Received 8th November 2010, Accepted 23rd November 2010

DOI: 10.1039/c0cp02460k

We have measured differential cross sections (DCSs) for the reaction $\text{H} + \text{D}_2 \rightarrow \text{HD}(v' = 2, j' = 0, 3, 6, 9) + \text{D}$ at center-of-mass collision energies E_{coll} of 1.25, 1.61, and 1.97 eV using the photoloc technique. The DCSs show a strong dependence on the product rotational quantum number. For the $\text{HD}(v' = 2, j' = 0)$ product, the DCS is bimodal but becomes oscillatory as the collision energy is increased. For the other product states, they are dominated by a single peak, which shifts from back to sideward scattering as j' increases, and they are in general less sensitive to changes in the collision energy. The experimental results are compared to quantum mechanical calculations and show good, but not fully quantitative agreement.

Introduction

The hydrogen exchange reaction $\text{H} + \text{H}_2 \rightarrow \text{H}_2 + \text{H}$ is the simplest neutral bimolecular reaction, and has for nearly a century served as a benchmark system in the field of reaction dynamics. It has thus been the focus of many experimental and theoretical efforts which have collectively provided a wealth of information on this system. Advances on both fronts, especially in the past two decades, have led to excellent agreement between the experimental measurements and calculations, and thus a sound understanding of the dynamics.¹ The reaction is known to be dominated by a direct-recoil mechanism proceeding through a collinear transition state geometry. The scattering is predominantly backwards for products with low rotational angular momentum j' , but becomes increasingly sideward as j' increases. In addition, over narrow ranges of collision energy, and products with low values of j' , the scattering has been observed to be forward-backward and even oscillatory.^{2–7} The origin of the forward scattering has been studied extensively by a number of different theoretical methods,^{8–11} and has been attributed to a second time-delayed mechanism in which the reactants proceed through a barrier bottleneck state on their way to products, while oscillations in the scattering are a result of interference between the two mechanisms.

Despite the long history, the measurement of state-to-state differential cross sections (DCSs), which provide the largest amount of dynamical information from scattering experiments, was not possible until the mid 1990s. These measurements have

proved to be technically challenging and many of these early studies suffered from either poor angular resolution, or a limited range of scattering angles. However, rapid advances in instrumentation have succeeded in improving this situation. Many DCS measurements^{12–20} presently show quantitative or near quantitative agreement with calculations, suggesting that all but the most subtle aspects of the dynamics for this system are well understood. Nonetheless, there are portions of the large parameter space of this reaction that remain unexplored, and filling these gaps is an important step toward completing our understanding of this fundamental system.

In this study we investigate the effect of collision energy on the DCSs for the $\text{H} + \text{D}_2 \rightarrow \text{HD}(v' = 2, j') + \text{D}$ reaction. The measured DCSs, obtained using the photoloc method, are compared to quantum mechanical (QM) calculations which are blurred according to our experimental conditions. We have selected four rotational states, $j' = 0, 3, 6$, and 9 , and three collision energies, 1.25, 1.61, and 1.97 eV, to sample a large range of the available parameter space, while keeping the number of experiments to a reasonable number. We find that not unlike our related collision energy dependence studies of $\text{H} + \text{D}_2 \rightarrow \text{HD}(v' = 1, j' = 2, 6, 10)$ ²¹ and $\text{H} + \text{D}_2 \rightarrow \text{HD}(v' = 3, j' = 0)$,⁶ the DCSs are highly sensitive to changes in the product rotational state, but less sensitive to changes in the collision energy, with the exception of $\text{HD}(v' = 2, j' = 0)$. For this product state, we observe clear signatures of interference between the direct-recoil and time-delayed mechanisms. Comparison of the QM calculations with the experimental results shows that they are in good agreement.

Experimental

This section presents only the details relevant to the present study as the apparatus used and its application in a similar

^a Department of Chemistry, Stanford University, Stanford, CA 94305-5080, USA. E-mail: zare@stanford.edu

^b Institut für Chemie, Universität Potsdam, Karl-Liebknecht-Strasse 24-25, 14476 Potsdam-Golm, Germany

^c Department of Chemistry, University of Cambridge, Lensfield Road, Cambridge CB2 1EW, UK

study have been thoroughly described elsewhere.^{21,22} Briefly, a mixture of 1–5% HBr in D₂ is supersonically expanded into the extraction region of a Wiley-McLaren time-of-flight (TOF) mass spectrometer through a pulsed valve (General Valve Series 9) operating at 10 Hz. The pressure behind the valve was maintained at around 1000–1200 Torr while the base pressure of the instrument is around 1×10^{-8} Torr. The expansion cools the reagents translationally and internally so that almost all of the D₂ molecules are prepared in ($v = 0, j \leq 2$). The molecular beam is intersected at right angles by two counterpropagating and focused linearly polarized UV laser beams, both with their electric field vectors pointing along the TOF axis. One of the two UV beams is used to initiate the reaction by photolyzing HBr at various wavelengths. This produces fast H atoms whose kinetic energy and spatial anisotropy is well-defined.^{21,23} The photolysis wavelengths used in this study are 199 nm, 214.3 nm, and 232.7 nm, corresponding to collision energies of 1.97, 1.61, and 1.25 eV, respectively. After a delay of 10–20 ns to allow for a single collision between reactants, the nascent HD products are state-selectively ionized by the second UV pulse ($\lambda = 216$ –220 nm) via [2 + 1] resonance-enhanced multiphoton ionization (REMPI) on the *Q*-branch members of the (2,0) band of the $E, F \ ^1\Sigma_g^+ - X \ ^1\Sigma_g^+$ transition. This delay is significant as it is long enough for an appreciable amount of products to build up while sufficiently short to prevent fly-out of products, thus preventing bias against fast-moving products. The nascent HD molecules are formed with speeds of 100–10 000 m s⁻¹ resulting in the Doppler broadening of the [2 + 1] REMPI lines. To ensure once again that products are detected without bias, the wavelength of the probe laser is incrementally scanned back and forth over the Doppler profile during the course of the experiment. Following ionization, the HD⁺ ions are accelerated using voltages $V_{\text{acc}} = -60$ V and $V_{\text{ext}} = -15$ V toward a position-sensitive delay line detector which records their three-dimensional velocity (V_x, V_y, V_z) as an ion image.

The largest source of difficulty in our measurement comes from the probe laser, which in a single laser pulse can both photolyze HBr to initiate the reaction and ionize HD products. This initiates reactions at an undesired collision energy, whose product velocity distributions typically overlap those that occurred at the intended collision energy. To overcome this problem, we alternate the delay between the photolysis and probe laser pulses on an every-other-shot basis. Half the time, the photolysis laser is fired before the probe laser, and reactions with both the intended and undesired collision energy take place; we call this our “two-laser signal.” The remainder of time, the photolysis laser is fired after the probe laser so that only reactions at the undesired collision energy take place, and we call this our “one-laser signal.” We acquired a total of 8000–15 000 ions after the subtraction of the one-laser signal from the two-laser signal for each product state at a specific collision energy. Each measurement is repeated three to five times over the course of two to five days to ensure good reproducibility. Finally, the three-dimensional velocity distributions are extracted from the ion images and then converted to a differential cross section (DCS) using the photoloc method.²¹

Theory

The quantum calculations of the DCSs were carried out using the wave packet method of ref. 24, in which a quantum wave packet, containing a spread of desired energies, is propagated from the initial (H + D₂) to the final (HD + D) arrangements of the reaction, on the potential energy surface of Boothroyd–Keogh–Martin–Peterson.²⁵ The propagation of the wave packet was partitioned into 3 stages, corresponding to the entrance, strong-interaction, and exit stages of its time evolution. The wave packet was represented on efficient basis sets constructed from grids based on (H + D₂) *Jacobi* coordinates in the reagent approach region, and (D + HD) coordinates in the transition-state and product exit regions. A separate propagation was carried out for each initial rotational quantum number $j = 0, 1, 2$ of the D₂ molecule, and for each value of its projection on the H + D₂ vector approach. The calculations were repeated for all partial waves in the range $J = 0$ –40, with the maximum projection of J on the intermolecular axis set to 30.

The different parameters used in our calculations were sufficient to yield state-to-state cross-sections converged to better than 1% over a continuous range of collision energies from 1.0 to 2.3 eV. The effects of the geometric phase and the coupling to the first excited electronic state were excluded from our calculations because these effects are known to be negligible over the range of collision energies considered.²⁶

Results

Differential cross sections have been measured for the H + D₂ → HD($v' = 2, j' = 0, 3, 6, 9$) + D reaction at center-of-mass collision energies of 1.25, 1.61, and 1.97 eV. At $E_{\text{coll}} = 1.25$ eV, we found that the ratio of two-laser to one-laser ions, as described above, was not large enough to obtain DCSs for the HD($v' = 2, j' = 6$) states. Additionally, the HD($v' = 2, j' = 9$) product is not energetically accessible at this collision energy. Each measured DCS is normalized to the corresponding calculated DCS integrated over the range of observed angles, and the results are presented in Fig. 1.

Fig. 1 also gives the calculated DCSs for all states studied at the different collision energies. These DCSs have undergone three sources of blurring to simulate the experimental conditions. The first accounts for the fact that our experimental conditions do not produce D₂ reactants in a single rotational state, but instead a distribution of primarily the initial rotational states $j = 0, 1, 2$. Therefore, the calculations, which are done in a strictly state-to-state manner, are weighted to account for this distribution. Additionally, neighboring DCSs then are summed over a 50 meV (fwhm) Gaussian distribution centered at the nominal collision energy to simulate imperfect translational cooling of the molecular beam.²⁷ Such a small spread in collision energy should have minimal effects on the DCS but should be more pronounced for low final rotational states where the variation with collision energy is faster. Indeed, this step had very little effect on the DCSs except in the case of $j' = 0$ at 1.25 eV where the agreement between theory and experiment was slightly improved. The calculated DCSs are then converted to speed distributions

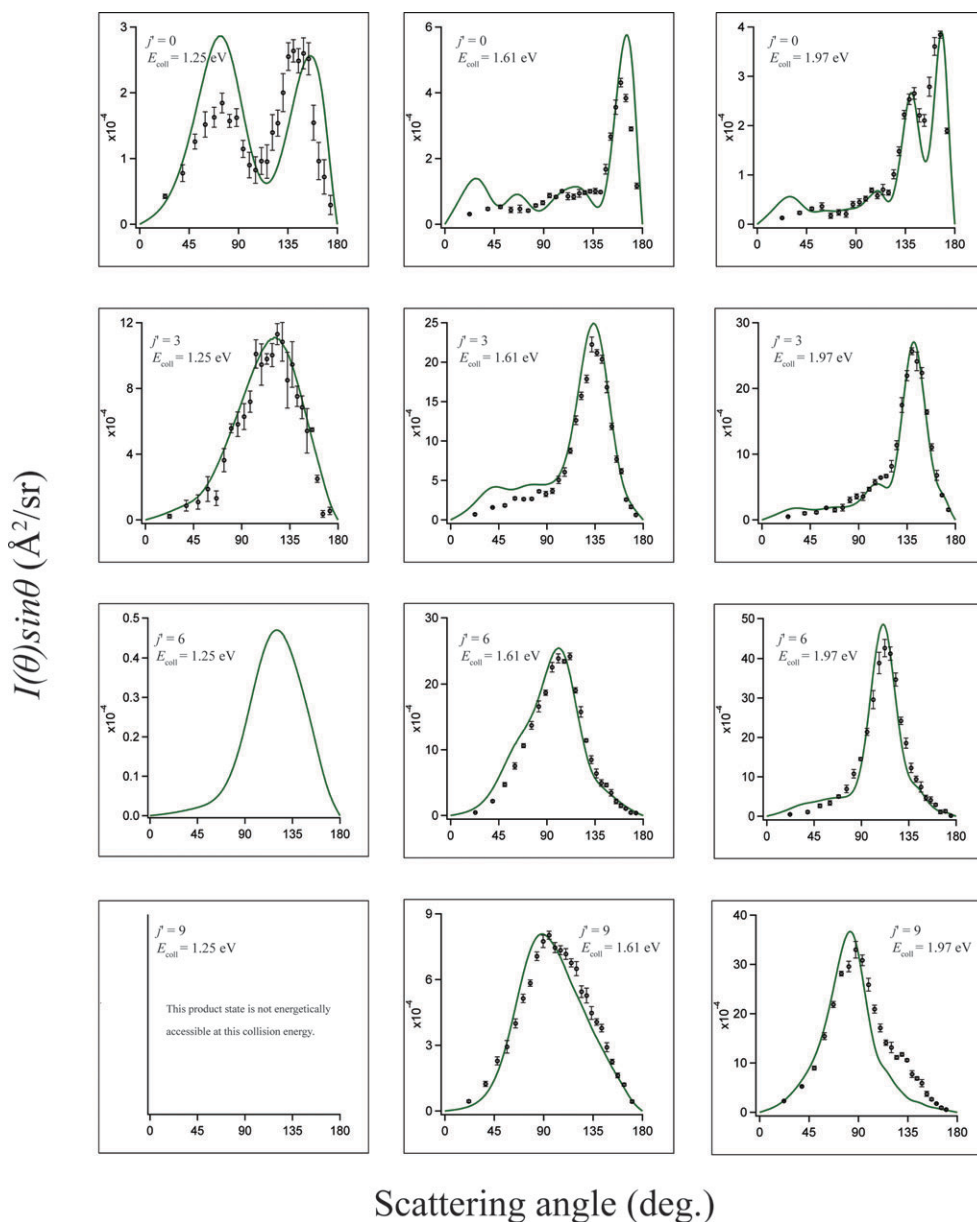


Fig. 1 Measurements (circles) and blurred calculations (solid lines) of the differential cross sections $I(\theta) \sin \theta$ for the HD($v' = 2, j' = 0, 3, 6, 9$) products formed from the H + D₂ reaction at various center-of-mass collision energies E_{coll} . The statistical error bars on the data represent one standard deviation from three to five repeated measurements.

using the law of cosines, and convoluted with a 500 m s⁻¹ (fwhm) Gaussian to simulate the finite instrumental resolution. Finally, the blurred speed distributions are converted back to DCSs. The main effect of this blurring is to wash out narrow oscillations which the resolution of our techniques prevent us from observing. Fig. 2 shows the result of the blurring on the raw calculations for the $j' = 0$ state at 1.61 eV.

It should also be noted that photolysis of HBr at the wavelengths used in this study proceeds by two channels, one producing ground-state Br ($^2P_{3/2}$) and one producing spin-orbit excited Br ($^2P_{1/2}$), commonly denoted Br*. In the latter, 0.45 eV (the spin-orbit energy) of the available energy is channeled into electronic excitation of the bromine atom rather than translation of the H atom. This channel thus produces H atoms with 0.36 eV less collision energy in the

center-of-mass frame. In our range of photolysis wavelengths (199–232.7 nm), this channel is a minor one with a branching fraction of a nearly constant $\Gamma = 0.16$. Additionally, collisions involving these slower H atoms with D₂ are less frequent and have a smaller reaction cross section. We therefore expect this channel to constitute a non-negligible but small contribution to our measurements and we have chosen to neglect it in this analysis. Furthermore, for experiments performed at a photolysis wavelength of 232.7 nm (fast-channel $E_{\text{coll}} = 1.25$ eV), collisions involving H atoms from the slow-channel produce HD($v' = 2, j' = 0$) with speeds that overlap only 5% of the fast-channel distribution (translating to roughly only one angular bin in the DCS), and are energetically unable to produce HD($v' = 2, j' = 3$). Slow-channel H atoms from photolysis at 214.3 nm (fast-channel $E_{\text{coll}} = 1.61$ eV) are

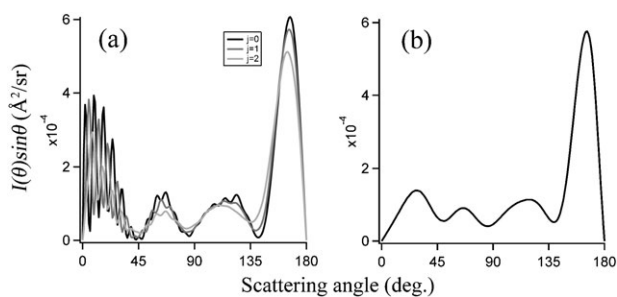


Fig. 2 An example of (a) raw and (b) blurred quantum mechanical calculations of the differential cross sections $I(\theta) \sin \theta$ for the $\text{HD}(v' = 2, j' = 0)$ product at $E_{\text{coll}} = 1.61$ eV. The calculations in (b) have undergone three sources of blurring which weight the DCSs from (a) according to the experimental initial distribution of rotational levels of the D_2 reagent, and account for imperfect reagent translational cooling and finite resolution of the instrument.

similarly unable to scatter into $\text{HD}(v' = 2, j' = 9)$ products because of energetic constraints. Please also note that we have chosen our collision energies such that the difference in energy is 0.36 eV between measurements, which corresponds to the difference in center-of-mass collision energy between H atoms from the fast and slow photolysis channels. For measurements in which both channels contribute to the DCS, the slow-channel subtraction methods of ref. 22 could be used, but again, we do not explore that in this analysis. The overall good agreement between theory and the experiment give us confidence in this choice.

Discussion

In Fig. 1 the blurred quantum mechanical calculations are compared to the experimentally measured DCSs. Overall, the agreement is good with the dominant features being observed in all cases. The close match gives us further confidence in both the experimental techniques and the ability of the theoretical methods to model the dynamics of this reaction.

The DCSs for $\text{HD}(v' = 2, j' = 0)$ as a function of collision energy are arguably the most interesting. At the lowest collision energy of 1.25 eV the scattering angle distribution is bimodal with the two broad maxima being of roughly equal magnitude. As the collision energy is increased to 1.61 eV, the backward scattered peak is narrowed and the maxima are shifted to larger angles. Broad oscillations in the forward and sideward regions of the DCS are present giving rise to three local maxima. Our data roughly follow these oscillations but the calculation predicts more intensity in the forward scattering region than was measured. At 1.97 eV the DCS is sharply double-peaked in the backward scattering region with a minor peak each in the sideward and forward scattered regions. Our experiment is able to resolve both backward scattered peaks and the sideward peak but under-measures the forward scattering.

We find that the agreement between the measurements and the calculations is good except in the case of $\text{HD}(v' = 2, j' = 0)$ at $E_{\text{coll}} = 1.25$ eV, the product state at the collision energy for which we have the least signal. We believe that the under-measurement of the broad side-scattered peak is an

experimental systematic error rather than a fault in the theory. These particular sets of data were the most challenging with the smallest signal, and highest ratio of interference from the REMPI laser, which became worse away from the center of the Doppler profile, *i.e.*, at larger speeds. We therefore found it difficult to scan over the entire Doppler profile without reducing our two-laser to one-laser signal ratio to 1. Consequently, products at the fastest speeds, and thus the smallest angles would be under-measured. A total of ten repeat measurements of the DCSs for this particular state were made, in two sets of five, separated by a period of over one month. Both of the data sets showed similar results, which indicates that the measurement is reproducible. We therefore suggest that the discrepancy is caused by an experimental systematic error. In spite of the failure of the experiment to match the theory quantitatively in all cases for $\text{HD}(v' = 2, j' = 0)$, we are pleased that the qualitative agreement is excellent with the major peaks in the scattering distribution being observed in the correct locations.

The large backward scattered peak is a result of the direct-recoil mechanism,^{28,29} which dominates the reaction for all but the lowest product rotational states. On the other hand, forward scattering in the $\text{H} + \text{D}_2$ reaction has been attributed to a time-delayed mechanism caused by the opening of an adiabatic barrier threshold⁷ (also referred to as a ‘quantum bottleneck state’). The system slows down as it passes over this threshold, which allows the temporarily associated atoms to rotate round, before scattering the products into the forward direction. This mechanism produces little rotational excitation of the product molecule, and therefore the forward scattering is observed only for low values of j' . The shapes and variation with collision energy of these DCSs are similar to those that were observed by Goldberg *et al.*⁶ for $\text{HD}(v' = 3, j' = 0)$ between 1.64 eV and 1.82 eV, though it should be noted that the collision energy range in the present study is much larger. We suggest that the forward scattering behavior for $\text{HD}(v' = 2, j' = 0)$ is the second instance of this type of scattering behavior, which can be termed a forward glory.³⁰ The forward-scattered peak is most intense at about $E_{\text{coll}} = 1.61$ eV. However, the energy-averaged DCS at 1.61 eV (Fig. 2b) shows only a modest forward-scattered peak because it averages over rapid oscillations caused by nearside–farside interference (see Fig. 2a).

As the product rotation is increased, the direct recoil mechanism rapidly takes over, and oscillations and forward scattering in the DCSs become less pronounced. This is clearly seen in the DCSs for $\text{HD}(v' = 2, j' = 3)$ which is primarily backscattered but shows a very small amount of forward scattering and oscillatory behavior. Our measurements are in good agreement with the calculations except at the smallest angles at $E_{\text{coll}} = 1.61$ eV, which again does not display as much forward scattering as the prediction. In both the calculated and measured DCSs for $\text{HD}(v' = 2, j' = 6, 9)$ only a single peak is observed, which indicates that direct recoil is the only mechanism at work. The agreement between the theory and experiment for these states is again satisfactory at all collision energies, but the measurement for $\text{HD}(v' = 2, j' = 9)$ at 1.97 eV is too high in the backscattered region of the DCS.

A couple more trends can be extracted from the data. For fixed collision energy, the backward scattered peaks are largely

shifted toward more intermediate angles as j' increases. This trend is clearly seen, for example, in the set of data taken at $E_{\text{coll}} = 1.61$ eV where the maxima of the backward scattered peak shifts from $\theta \approx 160^\circ$ for $j' = 0$ to $\theta \approx 90^\circ$ for $j' = 9$. This is associated with larger angular momentum of the reactants (*i.e.*, higher impact parameters) being channeled into higher rotational angular momentum, as well as leading to more glancing-type collisions. In contrast, with the exception of HD($v' = 2, j' = 0$) and to a very small extent HD($v' = 2, j' = 3$), increasing E_{coll} narrows the distributions but hardly changes the location or number of the maxima. This trend was observed in our previous DCSs measurements for the $v' = 1$ and $v' = 3$ manifolds as well.

In summary, experiment and theory are in close agreement for the $\text{H} + \text{D}_2 \rightarrow \text{HD}(v' = 2, j' = 0, 3, 6, 9) + \text{D}$ reaction at the center-of-mass collision energies studied. We do observe yet another example of forward glory scattering as the HD($v' = 2, j' = 0$) channel opens followed by interference between forward and backward scattering with increasing collision energy. Moreover, the glory scattering rapidly falls off as the rotational state of the product increases.

Acknowledgements

N.C.-M.B., J.J., T.G., and R.N.Z. acknowledge support from the US National Science Foundation under NSF CHE-1025960 and CHE-0650414-003. F.B. and S.C.A. acknowledge support from the UK Engineering and Physical Sciences Research Council.

References

- 1 F. J. Aoiz, L. Banares and V. J. Herrero, *Int. Rev. Phys. Chem.*, 2005, **24**, 119.
- 2 F. Fernandez-Alonso, B. D. Bean, A. E. Pomerantz, R. N. Zare and F. J. Aoiz, *Angew. Chem.*, 2000, **39**, 2748.
- 3 F. Fernandez-Alonso, B. D. Bean and R. N. Zare, *J. Chem. Phys.*, 2001, **115**, 4534.
- 4 J. D. Ayers, A. E. Pomerantz, F. Fernandez-Alonso, F. Austerfelder, B. D. Bean and R. N. Zare, *J. Chem. Phys.*, 2003, **119**, 4662.
- 5 A. E. Pomerantz, F. Austerfelder, R. N. Zare, S. C. Althorpe, F. J. Aoiz, L. Banares and J. F. Castillo, *J. Chem. Phys.*, 2004, **120**, 3244.
- 6 N. T. Goldberg, J. Zhang, D. J. Miller and R. N. Zare, *J. Phys. Chem. A.*, 2008, **112**, 9266.
- 7 S. A. Harich, D. Dai, C. C. Wang, X. Yang, S. D. Chao and R. Skodje, *Nature*, 2002, **419**, 281.
- 8 S. C. Althorpe, F. Fernandez-Alonso, B. D. Bean, J. D. Ayers, A. E. Pomerantz, R. N. Zare and E. Wrede, *Nature*, 2002, **416**, 67.
- 9 S. C. Althorpe, *J. Chem. Phys.*, 2002, **117**, 4623.
- 10 B. K. Kendrick, *J. Chem. Phys.*, 2001, **114**, 8796.
- 11 S. J. Greaves, D. Murdock and E. Wrede, *J. Chem. Phys.*, 2008, **128**, 116430.
- 12 F. Fernandez-Alonso, B. D. Bean and R. N. Zare, *J. Chem. Phys.*, 1999, **111**, 1022.
- 13 F. Fernandez-Alonso, B. D. Bean and R. N. Zare, *J. Chem. Phys.*, 1999, **111**, 1035.
- 14 F. Fernandez-Alonso, B. D. Bean and R. N. Zare, *J. Chem. Phys.*, 1999, **111**, 2490.
- 15 B. D. Bean, J. D. Ayers, F. Fernandez-Alonso and R. N. Zare, *J. Chem. Phys.*, 2002, **116**, 6634.
- 16 L. Schnieder, K. Seekamp-Rahn, J. Borkowski, E. Wrede, K. H. Welge, F. J. Aoiz, L. Banares, M. J. D'Mello, V. J. Herrero, V. Saez Rabanos and R. E. Wyatt, *Science*, 1996, **269**, 207.
- 17 L. Banares, F. J. Zoiz, V. J. Herero, M. J. D'Mello, B. Niederjohann, K. Seekamp-Rahn, E. Wrede and L. Schnieder, *J. Chem. Phys.*, 1998, **108**, 6160.
- 18 E. Wrede, L. Scheider, K. H. Welge, F. J. Aoiz, L. Banares, J. F. Castillo, B. Martinez-Haya and V. J. Herrero, *J. Chem. Phys.*, 1998, **110**, 9971.
- 19 S. A. Harich, D. Dai, X. Yang, S. D. Chao and R. T. Skodje, *J. Chem. Phys.*, 2002, **116**, 4769.
- 20 D. D. Dai, C. C. Wang, S. A. Harich, X. Wang, X. Yang, S. D. Chao and R. T. Skodje, *Science*, 2003, **300**, 1730.
- 21 K. Koszinowski, N. T. Goldberg, J. Zhang, R. N. Zare, F. Bouakline and S. C. Althorpe, *J. Chem. Phys.*, 2007, **127**, 124315.
- 22 K. Koszinowski, N. T. Goldberg, A. E. Pomerantz and R. N. Zare, *J. Chem. Phys.*, 2006, **125**, 133503.
- 23 P. M. Regan, S. R. Langford, A. J. Orr-Ewing and M. N. R. Ashfold, *J. Chem. Phys.*, 1999, **110**, 281.
- 24 S. C. Althorpe, *J. Chem. Phys.*, 2001, **114**, 1601.
- 25 A. I. Boothroyd, W. J. Keogh, P. G. Martin and M. R. Peterson, *J. Chem. Phys.*, 1996, **104**, 7139.
- 26 F. Bouakline, S. C. Althorpe and D. Peláez Ruiz, *J. Chem. Phys.*, 2008, **128**, 124322.
- 27 W. J. van der Zande, R. Zhang, R. N. Zare, K. G. McKendrick and J. J. Valentini, *J. Phys. Chem.*, 1991, **95**, 8205.
- 28 J. Hirschfelder, H. Eyring and B. Topley, *J. Chem. Phys.*, 1936, **4**, 170.
- 29 M. Karplus, R. N. Porter and R. D. Sharma, *J. Chem. Phys.*, 1965, **43**, 3259.
- 30 P. D. D. Monks, J. N. L. Connor and S. C. Althorpe, *J. Phys. Chem. A.*, 2007, **111**, 10302.